ELSEVIER

Journal of Hazardous Materials B73 (2000) 255–267

Journal of Hazardous Materials

www.elsevier.nl/locate/jhazmat

Investigation of the stability of hardened slag paste for the stabilization/solidification of wastes containing heavy metal ions

Chong Yoon Rha *, Seong Keun Kang, Chang Eun Kim

Department of Ceramic Engineering, Yonsei University, 134 Shinchon-dong, Seodaemoon-ku, Seoul 120-749, South Korea

Received 13 February 1998; received in revised form 15 October 1999; accepted 3 December 1999

Abstract

We have studied the effect of chromium ions and lead ions on the chemical stability of hardened slag paste with toxic wastes during the stabilization/solidification process. The influences of Cr and Pb ions on the hydration of slag were also investigated. Sodium silicate (Na_2SiO_3), 5 wt.% of slag, was used as an alkali activator for slag hydration. The physical stability of hardened paste containing partial replacement of slag with fly ash and gypsum was also examined.

When gypsum was added to slag, the compressive strength of hardened slag paste developed, accompanying the activation of alumino-ferrite–tricalciumsulfate (Al_2O_3-Fe_2O_3–$3CaSO_4$, AFt) and alumino-ferrite–monocalciumsulfate (Al_2O_3-Fe_2O_3–$CaSO_4$, AFm) phase generation. Those phases caused densification of the microstructure. Concurrently, the leaching amount of heavy metal ions was decreased. When fly ash was added to slag, the compressive strength increased and the leaching amount decreased with both active formation of aluminate hydrates and ion substitution. Lead ions were mostly stabilized through physical encapsulation by the hardened slag paste's hydrate matrix. In the case of chromium ions, we observed that it was mainly solidified through the formation of a substitutional solid solution with aluminum atoms in the structure of aluminate hydrates.

Keywords: Hardened slag paste; Chromium; Lead

* Corresponding author. Tel.: +82-2-361-2846.

0304-3894/00/$ - see front matter
PII: S0304-3894(99)00185-5

1. Introduction

Solidification is one of the recognized ways to dispose of sludge or water contaminated with toxic heavy metals. Solidification can be defined as the binder, such as slag, which either chemically binds toxic waste matter into solid bulks or physically cuts them off from the outside by forming a capsule. It is a process that converts potential toxic waste materials into less toxic solid materials before land filling [1]. Nowadays, solidification processes where cementitious or pozzolanic materials are used have been received as a good way to achieve solidification/stabilization. However, when ordinary Portland cement is used alone as a single binder, cost and the environmental requirements crop up as problems. For example, the cost of cement is much higher than that of slag and cement has a high pH value of up to 12.5–13.5. Thus, various attempts have been tried to replace cement with industrial by-products such as slag and fly ash [2].

Ground granulated blast-furnace slag (GGBS), a by-product of an iron foundry, is one of the available industrial by-products for the replacement of cement. Until recently, most of GGBS has been simply land-filled. Now, GGBS is welcomed as one of the raw materials for slag blended cement because of its latent hydraulic properties. However, the effect of heavy metal ion of waste materials on the hydration of slag and its solidification mechanism is still unknown. We have therefore studied the stabilization/solidification process of heavy metal ions in the slag system. In particular, we examined the influence of heavy metal ions, Pb and Cr ion, on the hydration of GGBS. We also studied the leaching characteristics and solidification mechanisms of hardened slag paste containing heavy metal ions.

2. Experimental

2.1. Starting materials and specimens

The blast furnace slag (Pohang Iron & Steel, Korea) with a fineness of 3483 cm^2/g, ordinary Portland cement (OPC, Ssangyong Cement, Korea) and fly ash (Boryung power station, Korea) were used. For the source of heavy metal ions, we used lead nitrate ($Pb(NO_3)_2$) and chromium(III) nitrate ($Cr(NO_3)_3 \cdot 8H_2O$). With a salts-to-binder ratio of 5 wt.%, the metal salts were dissolved into distilled water and batch mixed together. Sodium orthosilicate was added as an alkali activator to the slag in an aqueous phase with a ratio of 5 wt.% against the slag. The crystalline phase of the slag, as determined by X-ray diffraction, mainly included quartz, mullite, and spinel close to magnetite. The glass content of the fly ash, as determined by the quantitative X-ray diffractometer (QXRD, step scanning method), was about 65 wt.%. Chemical composition and fundamental physical properties of the starting materials are given in Tables 1–3. Adding water with a water/binder (W/B) ratio of 0.4 to slag blended cement, we fabricated cylindrical type (Φ30 mm $\times$ H40 mm) specimens. Specimens using fly ash and gypsum were also made in the same way. All specimens were cured at room

temperature and 100% relative humidity in the incubator for 3, 7, 14 and 28 days. Table 4 indicated the mixture design of all specimens used in this study.

2.2. Testing and analysis

The compressive strength was measured to evaluate the effect of Pb and Cr ions on the mechanical deviation of hardened slag paste according to the variation of its hydraulic properties. After this, the specimens were crushed to coarse powder and treated with an acetone–alcohol solution for stopping the hydration reaction. For the leaching test, the coarse powder after strength test was separated through a 9.5 mm sieve. An aqueous acetic acid solution ($pH = 2.88 \pm 0.05$) was used as a leaching solution. Two hundred milliliters of solution leached from every crushed specimen of 10 g was put into a polyethylene bottle and kept for 24 h at room temperature while being rotated at 30 rpm [1]. For the leached solution, heavy metal ion concentration was measured by inductively coupled plasma-atomic emission spectrometry (ICP-AES). For the remnant solid phase, sequential leaching tests with the new leaching solution were repeated.

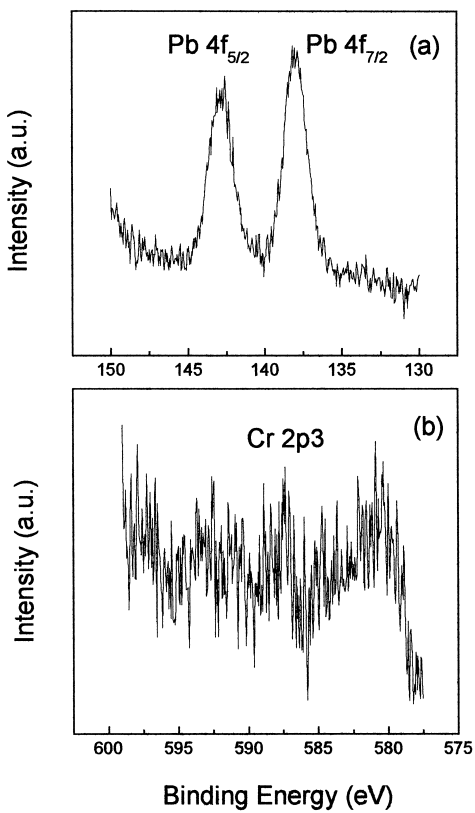

Fig. 1. XPS spectra of slag samples cured for 3 days. (a) Pb-doped sample — Pb^{2+} 4f line. (b) Cr-doped sample — Cr^{3+} 2p line.

3. Results and discussion

3.1. Effect of heavy metal ions on the hydration of slag

3.1.1. The rate of hydration

As heavy metal ions were added, the heat evolution curve and cumulative heat amount of slag paste till 72 h are shown in Fig. 4. Lead ion extremely retarded the heat evolution of slag paste. The second heat evolution appeared as late as 50 h. However, there was no retardation effect of Cr ion on the hydration of slag in the initial hydration period. It was considered that the Cr ion had two roles in the hydration reaction of slag. One is activating alumino-silicate gel involved in the initial strength development and concurrently restraining the formation of ettringite, which was known as a setting obstacle of calcium silicate in the initial hydration period. This could be a reasonable explanation for this phenomenon [3–5]. The other is a reaction forcing H_2O, a coordinator of complexing agent of Cr, to create substitution with OH^- in its liquid phase. Thus, chemical reaction of slag in a high alkali environment developed as follows:

$$Cr(H_2O)_6^{3+} \rightarrow Cr(OH)(H_2O)_5^{2+} \rightarrow Cr(OH)_3(H_2O)_3 \rightarrow Cr(OH)_4(OH)_2^{2-}$$

In the above reaction, H_2O was substituted by OH^- in the Cr complexing agent and OH concentration in water was reduced. Therefore, the effect of the alkali activator was diminished and the degree of hydration of slag was also decreased under Cr ion presence. As it was harder to break the Si—O or Al—O bond in a glass network of slag, the leached ion concentration in solution was also reduced and the amount of precipi-

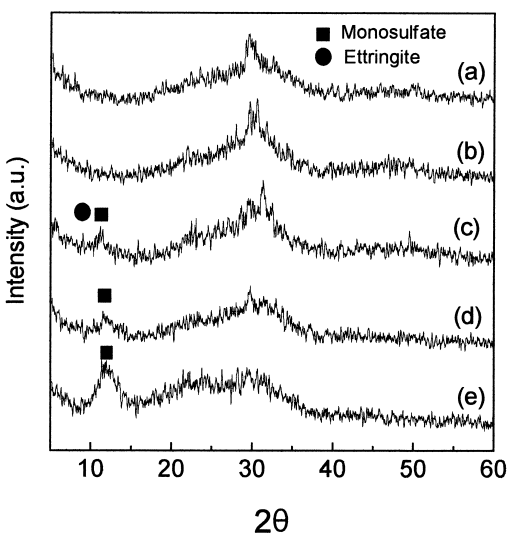

Fig. 2. XRD pattern of slag specimen cured for 14 days. (a) Slag, (b) Slag + Pb, (c) Slag + Gypsum + Pb, (d) Slag + Cr, (e) Slag + Flyash + Cr.

tated hydrates was reduced. On the other hand, the general retardation mechanism of Pb was attributed to an impermeable thin film, Pb salt, on slag particles. This explained why the hydration rate of slag paste with Pb ions is lower.

X-ray Photoelectron Spectroscopy (XPS) analysis results were shown in Fig. 5. The feature of Pb 4f line was quite clear but that of Cr 2p line appeared diversely. Considering that penetration depth of an enhanced photoelectron was approximately tens of angstroms, lead ion mainly existed on the slag surface. In other words, Pb ion in a liquid phase did not contribute to make the inner hydration products of slag but stayed only as a precipitator on the slag surface [6,7]. The binding energy of Pb $4f_{7/2}$ line shown in Fig. 1(a) was the closest to that of Pb $4f_{7/2}$ line in Pb–O bond. This meant lead ion concentrated on the surface of slag and precipitated into salts like hydroxides, carbonates, or sulfates. Because Pb salts had extremely low solubility, it was likely to work as a barrier between slag particle and water. For this reason, lead ion retarded the initial hydration of slag [8].

3.1.2. Variation of hydrates

To verify the variation of hydrates with heavy metal addition, X-ray diffraction analysis of 14-day hydrated specimens was done as shown in Fig. 2. XRD pattern of all

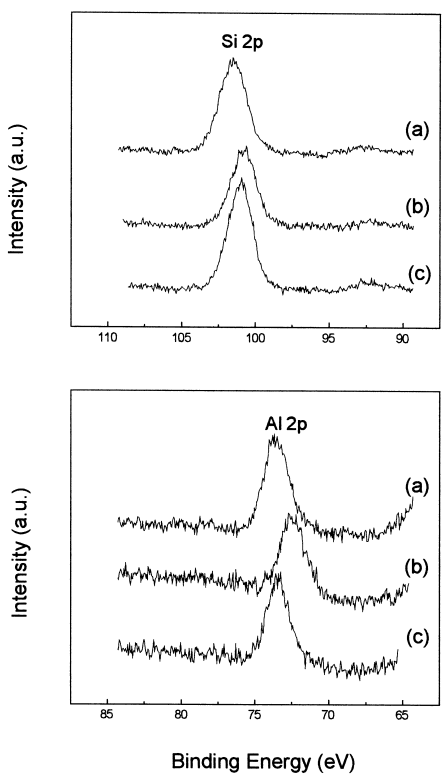

Fig. 3. XPS spectra of slag samples doped with Pb or Cr Si^{4+} 2p line and Al^{3+} 2p line. (a) Slag, (b) Slag + Pb, (c) Slag + Cr.

specimens indicated hydrates were low crystalline materials and peaks were overlapped due to diverse atomic spacing of hydrates, and thus showed a broad diffraction peak [9]. A halo appeared at around $2\theta = 30°–31°$ due to the glass structure ($CaO–Al_2O_3–MgO–SiO_2$) with a short-range order. We could observe a peak of type I calcium–silicate–hydrates with noncrystalline characteristic around 29° [10]. XRD pattern of hydrated slag specimen with lead ion was similar to that of neat slag specimen. XRD pattern of hardened slag + gypsum specimen with lead ion showed an etringite's peak around 9° and a mono-sulfate's peak between 11° and 12°. In XRD pattern (d), there was a monosulfate peak around 12°. XRD pattern of the slag + fly ash specimen with Cr showed that the intensity of the aluminate peak (etringite and monosulfate) increased. A broad peak having most similar location to that of $4CaO \cdot Al_2O_3 \cdot 13H_2O$ (C_4AH_{13})

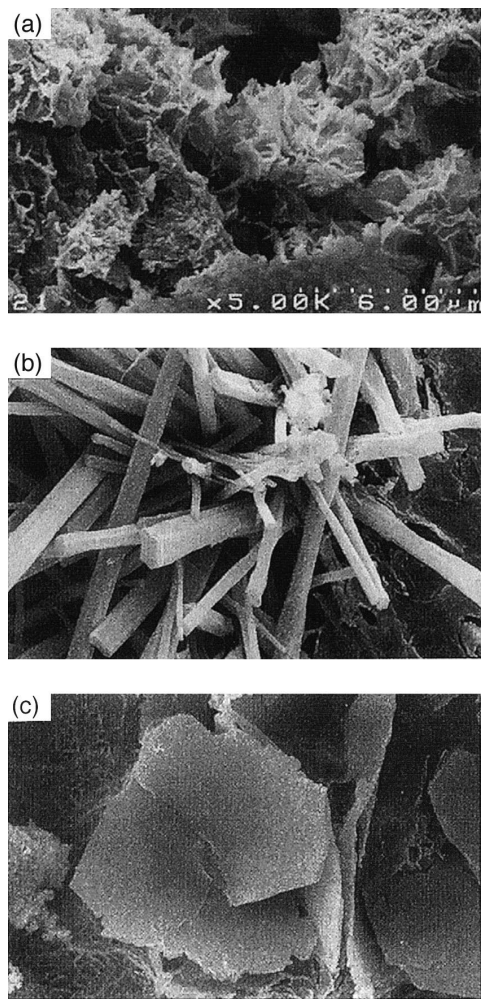

Fig. 4. SEM photograph of specimens cured for 14 days. (a) Slag, (b) Slag + Pb, (c) Slag + Cr.

was generated [11,12]. Through theses results, we could observe that Cr addition increased aluminate hydrates and broadened the diffused peak because Al^{3+} ion and Cr^{3+} ion generated a substitutional solid solution which consequently contained an irregular lattice parameter.

The result for binding energy of Si and Al analyzed by XPS was given in Fig. 3. The hydrated specimens for 14 days were also used. The binding energy of Si shifted to the lower side for Pb-doped slag specimen compared to that of neat slag or Cr-doped slag. Because SiO_4 tetrahedron in silica gel was corner shared with siloxane bond, the binding energy of Si atom was 104 eV, but the binding energy of Si atom in hydrates of slag specimen was shifted to the lower side [13]. In general, orthosilicate unit in calcium silicate hydrates of slag specimen formed cross-linked structure by polymerization, but Pb addition reduced the degree of silicate polymerization [14]. For slag + Pb specimen, therefore, binding energy of Si shifted to the lower side than that of neat slag specimen. In other words, 2 to 5 of SiO_4 tetrahedron generally made up Si polymer chains by sharing two vertices with each other but the addition of Pb ion meant it decreased the degree of silicate polymerization [15]. Al 2p line analysis showed that the binding energy of Al was lower for slag + Pb specimen, while the binding energy of Cr was relatively higher for slag + Cr specimen. It was considered that Al ion in slag particles primarily formed alumino-ferrite trisulfate/alumino-ferrite monosulfate (AFt/Afm) phase but Cr ion generated calcium–aluminium–hydrates with chain structure.

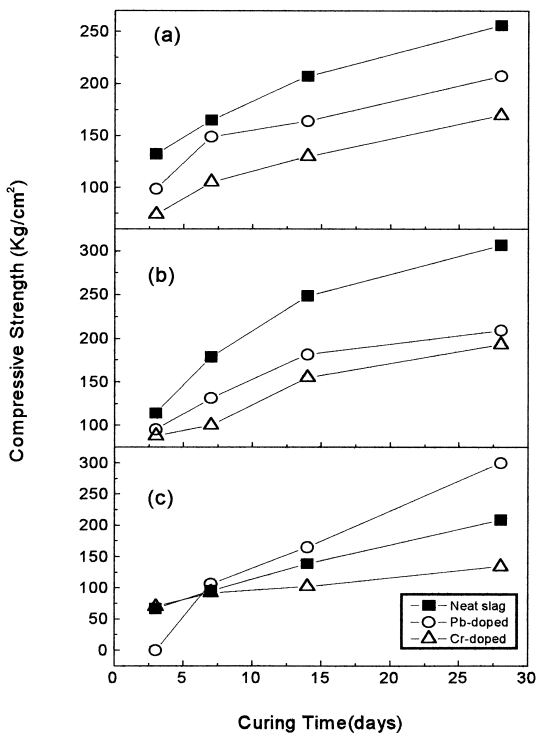

Fig. 5. Compressive strength as the function of curing days. (a) Slag, (b) Slag + Fly ash, (c) Slag + Gypsum.

Microstructural photographs of hardened slag paste for 14 days by scanning electron microscope (SEM) were shown in Fig. 4. Pores of hardened slag specimen were filled with large content of hydrates due to alkali activation by sodium silicate. Especially, we could observe honeycomb like C–S–H (II). One of the striking features of hardened slag paste with Pb was the rod shaped calcium–alumino-hydrate (ettringite) crystal. The other was the film by Pb salt present in the dark area. Impermeable thin film by an insoluble Pb salt was considered to retard the hydration of silicate hydrates in common. These effects were suspicious for the precipitation of hydrates in calcium–sulpho-aluminate system. In the picture (c) of hardened slag paste with Cr, there occurred a distinct generation of plate shaped calcium–alumino-hydrates (monosulfate).

3.2. Characteristics of heavy metal ions in hardened slag paste

3.2.1. Compressive strength

The measured compressive strengths of hydrated specimens for 3, 7, 14 and 28 days with and without 5 wt.% lead or Cr ions of solid in the nitrate form are given in Fig.

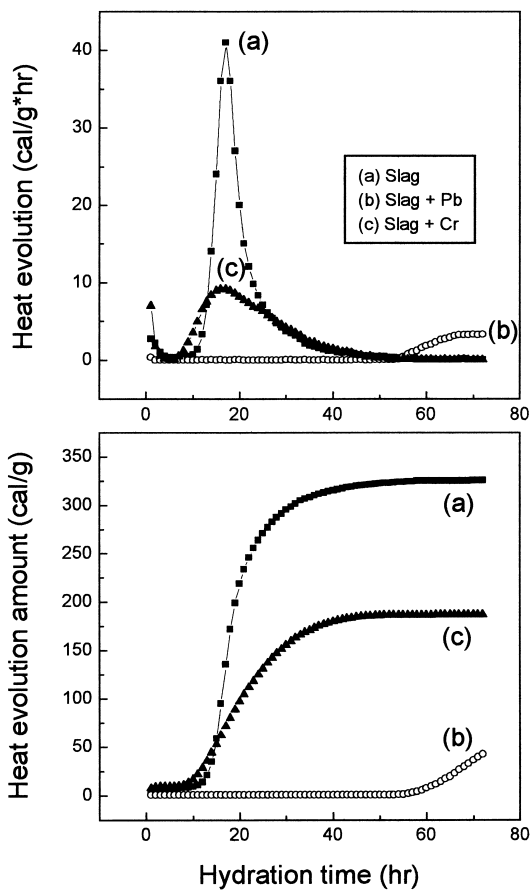

Fig. 6. Heat evolution of hydration of slag doped with heavy metal.

5(a,b and c) for slag, slag + fly ash and slag + gypsum, respectively. In all three cases listed above, the compressive strength of hardened paste with heavy metal ion was less developed than that of the hardened slag paste. It is thought that the changed pore structure originating from latent hydraulic property of slag or unstable hydrates created by modified hydration process was the main cause of the lower development of compressive strength [16]. In particular Cr ion weakened the structure of slag paste more than lead ion did. In any case, the values of compressive strengths of all specimens after a 3-day curing were enough to meet the land filling standard of 10 kg/cm^2 [17].

In graph (a), the development of compressive strength was still lasting due to the formation of hydrates caused by the sodium silicate as an alkali activator. As Pb or Cr ion was added, the compressive strength value of the slag sample was lower than that of the neat slag sample. It was because the hydration rate was quite slow in the initial reaction period for Pb ion addition. In the case of Cr ion addition, a large influence on the hydration of slag was not expected and retarded hydration in its initial reaction period was not detected as shown in Fig. 6. However, compressive strength value of Cr-doped slag sample was merely half that of the neat slag sample and showed slower strength development. The result of compressive strength of hardened slag + fly ash paste samples was similar to that of the hardened slag paste. The difference between the values of compressive strength of Pb-doped and Cr-doped sample was very small. In graph (c), the initial strength value of Pb-doped sample was too low to be measured but

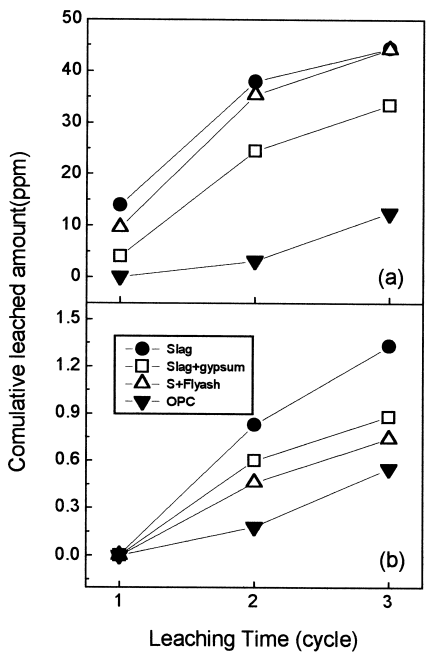

Fig. 7. Ion concentration of leachate after subsequent leaching test. (a) Pb ion concentration of Pb-doped slag, (b) Cr ion concentration of Cr-doped slag, OPC; ordinary Portland cement.

thereafter the strength increased sharply. Pb-doped sample had greater value of compressive strength than that of specimens with no heavy metal ions at the 14th day.

3.2.2. Leaching test

The leaching test for heavy metal doped samples was done for 24 h in an aqueous acetic acid solution (pH = 2.88 ± 0.05) [18] and the cumulative concentration of leached heavy metal ions from the 14-day hydrated specimen is shown in Fig. 7. In the Pb-doped system, leached Pb concentration from the hardened slag + gypsum sample was distinctly lower than that of the slag sample. In the Cr-doped system, the leached amount of Cr ion showed the lowest value for the hardened slag + fly ash paste except when the ordinary Portland cement (OPC) paste was used as reference.

Pore size distribution of the different slag combinations with Pb is shown in Fig. 8. Instead for the micropores of hardened slag + Pb paste to drastically decreas, macropores around 0.1 μm made up the mean pores. It was considered that the hydration of slag was changed as the Pb ion was added to the slag. In the case of the hardened slag + gypsum paste with Pb ion, however, the incremental volume of micro-pores

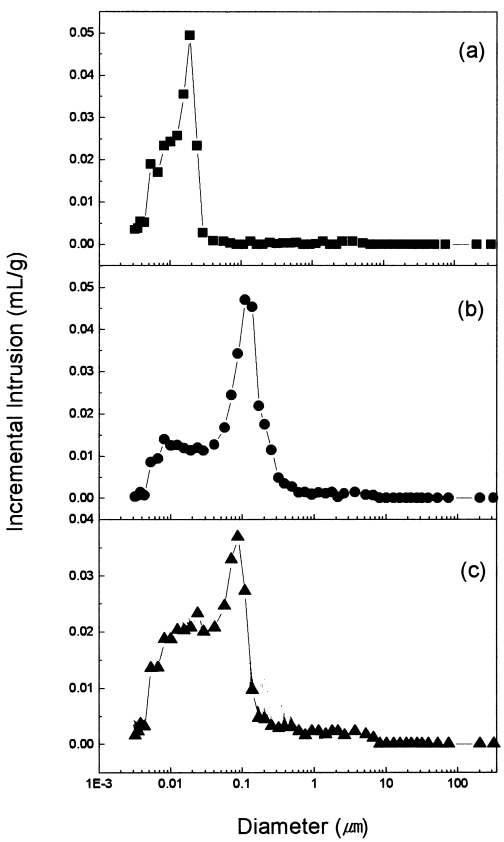

Fig. 8. Pore size distribution of specimen cured for 14 days. (a) Slag, (b) Slag + Pb, (c) Slag + Gypsum + Pb.

around 0.01 μm was substantially higher compared to that of the slag + Pb samples. A remarkable increase in micro-pore could be explained by the active formation of hydrates like the AFm and ettringite-containing SO_4^{2-} produced by gypsum.

Pore size distribution of the different slag combinations with Cr is shown in Fig. 9. For the hardened Cr-doped slag paste, macropores having a pore diameter of around 0.1 μm that were absent from slag-only specimens existed. For the hardened Cr-doped slag + fly ash paste, pores having two different sizes were observed; one smaller group centered around 0.1 μm and a larger group centered around 0.01 μm. This phenomenon could be attributed to either the hydrates generated from fly ash or dense microstructure by the active pozzolanic reaction of Cr ion.

Consequently, gypsum and fly ash of samples inhibited leaching of Pb and Cr, respectively. Both of them filled the micro-pores of hardened paste and limited the generation of open pore. Eventually, by developing a tortuous pore structure, we could reduce the leached amount of heavy metal ion when the hardened paste contacted a leaching solution.

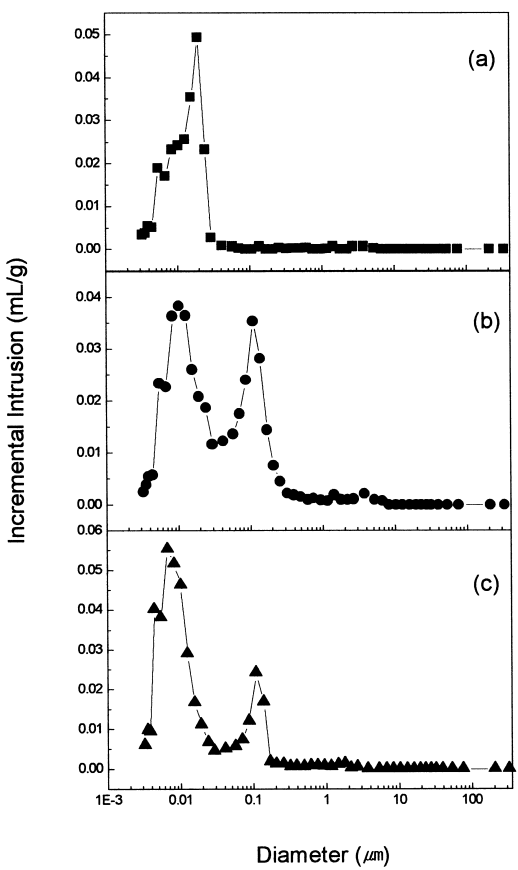

Fig. 9. Pore size distribution of specimen cured for 14 days. (a) Slag, (b) Slag + Cr, (c) Slag + Fly ash + Cr.

4. Conclusion

From the above results we conclude the following points.

(a) Lead ions retarded the hydration of slag because they formed an insoluble and impermeable thin film. The film around the slag particle interrupted the reaction between water and slag surface. Solidification of lead ions is therefore due to the physical encapsulation by the hydrate matrix.

(b) Gypsum induced the structural densification of slag through the formation of AFt and AFm phase. Therefore, the value of compressive strength increased and lead ion leaching amount decreased.

(c) Chromium ions accelerated the initial hydration of slag and generated aluminate hydrates. Subsequently, the degree of hydration decreased as hydroxy ions were consumed as a complexing agent of chromium in the pore solution. Therefore, the effect of alkali activator was reduced. Stabilization of chromium ions was mainly due to the substitution of calcium aluminate hydrates.

(d) By using gypsum or fly ash, compressive strength increased via the active generation and substitution of aluminate hydrates. Hoewever, the leaching amount of chromium ions decreased.

References

[1] M.D. LaGrega, P.L. Buckingham, J.C. Evans, in: Hazardous Waste Management, Mcgraw-Hill International editions, 1994, p. 641.
[2] E. Douglas et al., A preliminary study on the alkali activation of ground granulated blast-furnace slag, Cem. Concr. Res. 20 (1990) 746–756.
[3] J.R. Conner, in: Chemical Fixation and Solidification of Hazardous Wastes, Van Nostrand-Reinhold, 1990, p. 638.
[4] V.A. Rossetti et al., Inertization of toxic metals in cement matrices: effects on hydration, setting and hardening, Cem. Concr. Res. 25 (6) (1995) 1147–1152.
[5] D.G. Ivey et al., Electron microscopy of heavy metal waste in cement matrices, J. Mater. Sci. 25 (1990) 5055–5062.
[6] K.S. Jun et al., Microstructural analysis of OPC/silica fume/Na-bentonite interactions in cement based solidification of organic-contaminated hazardous waste, J. Environ. Sci. Health 32 (4) (1997) 913–928.
[7] H.G. Mcwhinney et al., An investigation of mercury solidification and stabilization in Portland cement using X-ray photoelectron spectroscopy and energy dispersive spectroscopy, Cem. Concr. Res. 20 (1990) 79–91.
[8] D. Cocke et al., A model for lead retardation of cement setting, Cem. Concr. Res. 19 (1989) 155–159.
[9] A. Roy et al., Activation of ground blast-furnace slag by alkali-metal and alkali earth hydroxides, J. Am. Ceram. Soc. 75 (12) (1992) 3233–3240.
[10] S.D. Wang, K.L. Scrivener, Hydration products of alkali activated slag cement, Cem. Concr. Res. 25 (3) (1995) 561–571.
[11] C.D. Hills et al., Solidification of hazardous wastes containing cyanide, Cem. Concr. Res. 24 (4) (1994) 707–714.
[12] J.D. Ortego et al., Solidification of hazardous substances — a TGA and FTIR study of Portland cement containing metal nitrates, J. Environ. Sci. Health A 24 (6) (1989) 589–602.
[13] M. Yousuf, A. Mollah et al., An FTIR and XPS investigations of the effects of carbonation on the solidification/stabilization of cement based systems — Portland type V with zinc, Cem. Concr. Res. 23 (1993) 773–784.

[14] M. Yousuf, A. Mollah et al., Surface and bulk studies of leached and unleached fly ash using XPS, SEM, EDS and FTIR techniques, Cem. Concr. Res. 24 (1994) 109–118.
[15] D. Viehl et al., Mesostructure of calcium silicate hydrate (C–S–H) gels in Portland cement paste: short range ordering, nanocrystallinity, and local compositional order, J. Am. Ceram. Soc. 79 (7) (1996) 1731–1744.
[16] J. Jambor, Pore structure and strength development of cement composites, Cem. Concr. Res. 20 (1990) 948–954.
[17] Gordon, C.C. Yang et al., Further study on properties of a solidified electroplating sludge using a mixture of an electroplating sludge and a calcium carbonate sludge as a binder, J. Hazard. Mater. 39 (1994) 301–315.
[18] G.C. Bye, in: Portland Cement: Composition, Production and Properties, Pergamon, 1983, p. 116.